Macromolecules

Article

Synthesis and Self-Assembly of Coil#Rod Double Hydrophilic Diblock Copolymer with Dually Responsive Asymmetric Centipede-Shaped Polymer Brush as the Rod Segment

Changhua Li, Zhishen Ge, Jin Fang, and Shiyong Liu

Macromolecules, **2009**, 42 (8), 2916-2924• DOI: 10.1021/ma900165z • Publication Date (Web): 25 March 2009

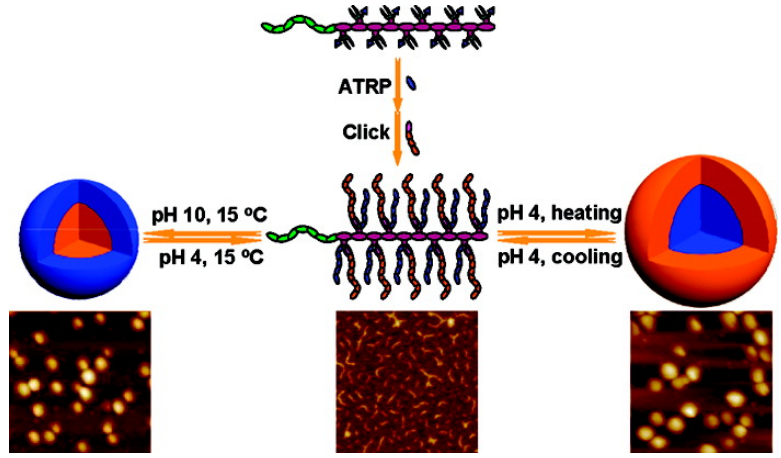

More About This Article

Additional resources and features associated with this article are available within the HTML version:

- Supporting Information
- Access to high resolution figures
- Links to articles and content related to this article
- Copyright permission to reproduce figures and/or text from this article

View the Full Text HTML

Macromolecules is published by the American Chemical Society. 1155 Sixteenth Street N.W., Washington, DC 20036

Synthesis and Self-Assembly of Coil−Rod Double Hydrophilic Diblock Copolymer with Dually Responsive Asymmetric Centipede-Shaped Polymer Brush as the Rod Segment

Changhua Li, Zhishen Ge, Jin Fang, and Shiyong Liu*

CAS Key Laboratory of Soft Matter Chemistry, Department of Polymer Science and Engineering, Hefei National Laboratory for Physical Sciences at the Microscale, University of Science and Technology of China, Hefei, Anhui 230026, China

Received January 24, 2009; Revised Manuscript Received March 9, 2009

ABSTRACT: We report on the synthesis and self-assembly of well-defined coil−rod double hydrophilic diblock copolymer with pH- and thermo-responsive asymmetric centipede-shaped polymer brush as the rod segment via a combination of atom transfer radical polymerization (ATRP) and click chemistry (Schemes 1 and 2). At first, poly(ethylene oxide)-*b*-poly(glycidyl methacrylate), PEO-*b*-PGMA, was prepared by ATRP using PEO-based macroinitiator. The ring-opening of pendent epoxide moieties in PEO-*b*-PGMA with NaN_3 followed by esterification with 2-bromoisobutyryl bromide afforded multifunctional PEO-*b*-[PGMA-(N_3)(*Br*)] bearing one azide and one bromine moieties on each monomer repeating unit of PGMA. The subsequent ATRP of 2-(2-methoxyethoxy)ethyl methacrylate (MEO_2MA) using PEO-*b*-[PGMA-(N_3)(*Br*)] as the macroinitiator yielded PEO-*b*-[PGMA-*g*-(N_3)($PMEO_2MA$)] coil−brush diblock copolymer possessing one residual azide moiety at each grafting site. Finally, the target coil−rod diblock copolymer with asymmetric centipede-shaped polymer brush as the rod segment, PEO-*b*-[PGMA-*g*-(PDEA)($PMEO_2MA$)], was obtained via the click reaction of PEO-*b*-[PGMA-*g*-(N_3)-($PMEO_2MA$)] with an excess of alkynyl-terminated poly(2-(diethylamino)ethyl methacrylate) (*alkynyl*-PDEA). All the intermediate and final products were characterized by ^1H NMR, Fourier transform infrared spectroscopy (FT-IR), and gel permeation chromatography (GPC). Atomic force microscopy (AFM) analysis revealed that PEO-*b*-[PGMA-*g*-(PDEA)($PMEO_2MA$)] coil−rod diblock unimer chains adopt a wormlike conformation in aqueous solution at pH 4 and room temperature. Possessing pH-responsive PDEA and thermo-responsive $PMEO_2MA$ grafts arranged in an asymmetric centipede manner within the rod segment, PEO-*b*-[PGMA-*g*-(PDEA)($PMEO_2MA$)] self-assembles into two types spherical aggregates in aqueous solution, depending on solution pH and temperatures. The multiresponsive switching between wormlike unimers and two types of micellar aggregates were characterized by temperature-dependent optical transmittance, dynamic laser light scattering (LLS), AFM, and transmission electron microscopy (TEM).

Introduction

Stimuli-responsive double hydrophilic block copolymers (DHBCs) have attracted ever-increasing attention in the past decade due to their promising applications as drug and gene nanocarriers, sensors, smart actuators, and catalysis.[1−13] Certain DHBCs can supramolecularly self-assemble into more than one type of aggregates, i.e., so-called "schizophrenic" aggregation, in aqueous solution upon properly tuning external conditions such as pH, temperature, and ionic strengths.[1,6,9,14−28] In particular, recent developments in this field involve DHBCs possessing nonlinear chain topology. It has been well-established that chain architectures of block copolymers can dramatically affect their microphase separation patterns in bulk states and at interface as well as supramolecular aggregation properties in selective solvents.[9,29−33]

The first report of nonlinear DHBC was reported by Armes et al., concerning the synthesis Y-shaped AB_2 miktoarm star copolymers and their stimuli-responsive aggregation in aqueous solution.[34−36] Recently, we also reported the synthesis and self-assembly of nonlinear DHBCs possessing AB_4, A_2BA_2 H-shaped, and A_4BA_4 super-H-shaped architectures.[37,38] It is worthy of noting that previous examples of linear and nonlinear DHBCs typically consist of more than one type of linear flexible chain segments, which adopt random coil conformations when molecularly dissolved in water. On the other hand, if a high density of side chains is covalently attached to linear backbones, the so-called polymer brushes will take an extended cylindrical conformation. It can be envisaged that structural motif of rodlike polymer brush will endow nonlinear DHBCs with extra architectural versatility and more intriguing aggregation properties.

Comb-shaped polymer brushes can be categorized into homopolymer brushes[39−43] and copolymer brushes.[44−60] The latter typically consist of two or more types of polymer side chains. When only two types of polymer grafts are involved, they can be arranged in a random,[44,45] alternating,[46−48] block,[49−53] and "centipede" manner.[54−59] The synthesis of homopolymer and copolymer brushes can be achieved via grafting-through,[46−48,61] grafting-from,[50,52,55,59] and grafting-onto[44,45,62−65] techniques. Starting from macroinitiators with initiating sites distributed on each monomer repeating unit, the recent boom of controlled polymerization techniques, such as ring-opening polymerization (ROP),[45,46,59] nitroxide-mediated polymerization (NMP),[60,66] atom transfer radical polymerization (ATRP),[41,42,50,52,54,55] and reversible addition−fragmentation chain transfer (RAFT) polymerization,[51,67] have rendered the grafting-from approach more prevailing.

Chen et al.[42] reported the synthesis of coil−rod DHBCs with pH-responsive comb-shaped polymer brushes possessing poly(methacrylic acid) (PMAA) side chains as the rod segment via consecutive ATRP and investigated their application as crystallization mediators. Huang et al.[41] recently reported the synthesis of multiresponsive coil−rod DHBCs consisting of thermoresponsive poly(*N*-isopropylacrylamide) (PNIPAM) coil segment and pH-responsive poly(2-(diethylamino)ethyl methacrylate) (PDEA) brush as the rod segment. In the above two examples

* To whom correspondence should be addressed. E-mail: sliu@ustc.edu.cn.

10.1021/ma900165z CCC: $40.75
Published on Web 03/25/2009

Scheme 1. Synthetic Routes Employed for the Synthesis of Well-Defined Coil−Rod Double Hydrophilic Diblock Copolymer with pH- and Thermo-responsive Asymmetric Centipede-Shaped Polymer Brush As the Rod Segment, PEO-*b*-[PGMA-*g*-(PDEA)(PMEO$_2$MA)], via a Combination of ATRP and Click Chemistry

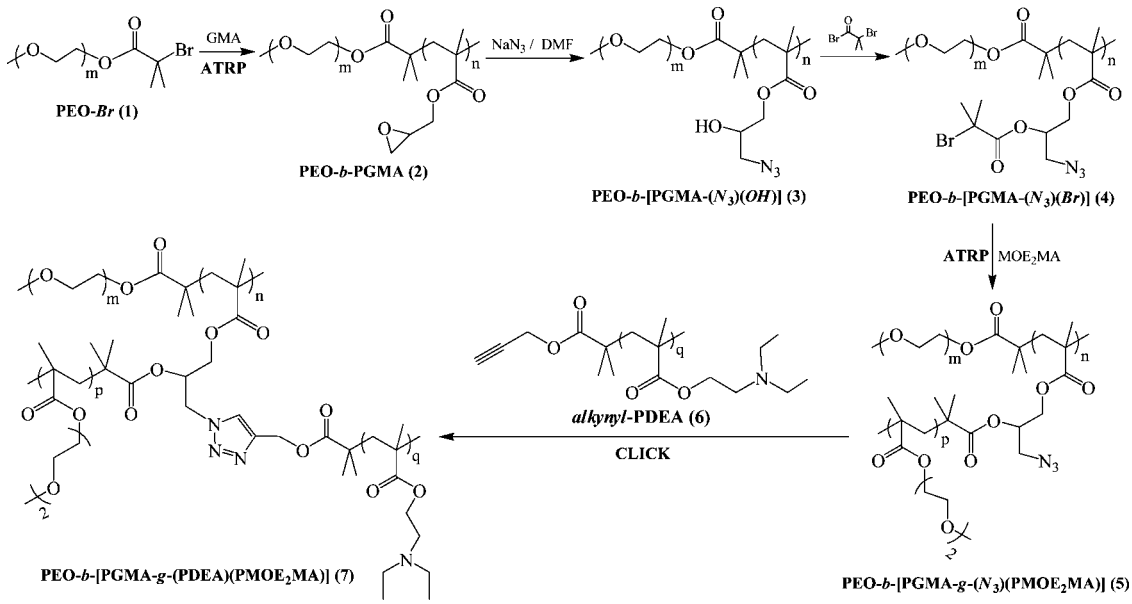

Scheme 2. Schematic Illustration of the Synthesis and Multi-responsive Supramolecular Self-Assembly of Coil−Rod Double Hydrophilic Diblock Copolymer, PEO-*b*-[PGMA-*g*-(PDEA)(PMEO$_2$MA)]

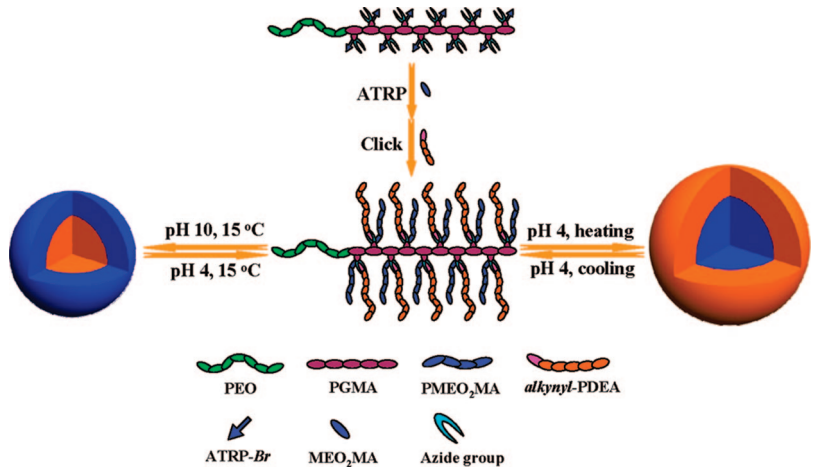

concerning coil−rod DHBCs, the rod segments are homopolymer brushes. Most recently, Huang et al.[54] also reported the synthesis of pH-responsive asymmetric centipede-shaped DHBCs possessing PMAA and short poly(ethylene oxide) (PEO) side chains via two successive ATRP processes.

Recently, the concept of click chemistry invented by Sharpless et al.[68,69] has also been introduced into the synthesis of polymer brushes.[40,62−65] Fréchet and Hawker et al.[62] successfully prepared rodlike dendronized polymer brushes via click reaction of poly(vinyl acetylene) with azide-functionalized dendrons. It was found that quantitative click grafting can be achieved for dendrons up to the third generation. Matyjaszewski and coworkers[64] reported the synthesis of polymer brushes by the click reaction between alkynyl-functionalized poly(2-hydroxyethyl methacrylate) (PHEMA) and monoazide-terminated polymers, and the grafting efficiency can be up to 88.4% for short PEO-N_3 precursors. Very recently, Huang et al.[65] successfully synthesized a novel type of polymer brush via click reaction, starting from ABC miktoarm star terpolymer possessing a clickable functionality at one of the arm terminal, and a grafting efficiency of 63.9% was achieved.

To the best of our knowledge, the concept of click chemistry has not been applied to the synthesis of nonlinear coil−rod DHBCs with multiresponsive centipede-shaped polymer brush as one of the building blocks. In this work, we report on the synthesis and self-assembly of well-defined double hydrophilic coil−rod diblock copolymer possessing dually responsive asymmetric centipede-shaped polymer brush as the rod segment (Schemes 1 and 2). At first, poly(ethylene oxide)-*b*-poly(glycidyl methacrylate), PEO-*b*-PGMA, and monoalkynyl-terminated PDEA, *alkynyl*-PDEA, were prepared via the ATRP technique. The ring-opening reaction of pendent epoxide moieties of PGMA segment with NaN_3 and subsequent esterification with 2-bromoisobutyryl bromide afforded the multifunctional initiator, PEO-*b*-[PGMA-(N_3)(*Br*)], bearing one azide and one bromine moiety on each monomer repeating unit within the PGMA segment. The synthesis of PEO-*b*-[PGMA-*g*-(PDEA)-(PMEO$_2$MA)] was accomplished by the ATRP of 2-(2-methoxyethoxy)ethyl methacrylate (MEO$_2$MA) monomer using PEO-*b*-[PGMA-(N_3)(*Br*)] as the macroinitiator, followed by click reaction of the obtained PEO-*b*-[PGMA-*g*-(N_3)(PMEO$_2$MA)] with an excess of *alkynyl*-PDEA. Possessing pH- and thermo-

responsive PDEA and $PMEO_2MA$ side chains arranged in an asymmetric centipede manner within the rod segment, the multiresponsive aggregation behavior of PEO-*b*-[PGMA-*g*-(PDEA)($PMEO_2MA$)] in aqueous solution has been further investigated.

Experimental Section

Materials. Poly(ethylene oxide) monomethyl ether (PEO_{113}-OH, M_n = 5.0 kDa, M_w/M_n = 1.06, mean degree of polymerization, DP, is 113) and 2,2′-bipyridine (bpy, 99% purity) were purchased from Aldrich and used as received. Glycidyl methacrylate (GMA, 98%, Aldrich), 2-(2-methoxyethoxy)ethyl methacrylate (MEO_2MA, 99%, Aldrich), and 2-(diethylamino)ethyl methacrylate (DEA, 99%, Aldrich) were dried over calcium hydride, vacuum-distilled, purged with nitrogen, and stored at −20 °C prior to use. *N,N,N′,N″,N″*-Pentamethyldiethylenetriamine (PMDETA, 99%, Aldrich), 2-bromoisobutyryl bromide (98%, Aldrich), copper(I) bromide (CuBr, 98%, Aldrich), copper(I) chloride (CuCl, 99.995%, Aldrich), sodium azide (NaN_3, 99%, Alfa Aesar), and tributyltin hydride (97%, Acros) were used as received without further purification. Merrifield Resin was purchased from GL Biochem (Shanghai) Ltd. and used as received. Triethylamine (TEA), isopropyl alcohol (IPA), and toluene were dried over CaH_2 and distilled at reduced pressure. Ammonium chloride (NH_4Cl), copper(II) dichloride ($CuCl_2$), *N,N*-dimethylformamide (DMF), propargyl alcohol, and all other chemicals were purchased from Sinopharm Chemical Reagent Co. Ltd. and used as received. Azido-functionalized Merrifield resin[70] and propargyl 2-bromoisobutyrate (PBIB)[71,72] were prepared according to literature procedures.

Synthetic schemes employed for the preparation of coil−rod double hydrophilic diblock copolymer with dually responsive asymmetric centipede-shaped polymer brush as the rod segment, PEO-*b*-[PGMA-*g*-(PDEA)($PMEO_2MA$)], are shown in Schemes 1 and 2.

Preparation of PEO-Br Macroinitiator (1). A typical procedure employed for the preparation of **1** was as follows. PEO_{113}-OH (15.0 g, 3.0 mmol) was dissolved in 250 mL of dry toluene upon heating. After azeotropic distillation of 60−80 mL of toluene at reduced pressure to remove traces of water, triethylamine (0.46 g, 4.5 mmol) was added, and the mixture was cooled to 0 °C in an ice−water bath. Under stirring, 2-bromoisobutyryl bromide (1.03 g, 4.5 mmol) in 30 mL of dry toluene was added dropwise over 1 h. The reaction mixture was stirred at room temperature overnight. After filtration, the filtrates were evaporated to dryness on a rotary evaporator. The residues were dissolved in 200 mL of CH_2Cl_2 and extracted with saturated $NaHCO_3$ aqueous solution (3 × 50 mL). The organic phase was then dried over anhydrous Na_2SO_4 and treated with activated charcoal. After filtration, the filtrates were precipitated into an excess of *n*-hexane. After drying in a vacuum oven overnight at room temperature, **1** was obtained as a white solid (14.23 g, yield: 92%; $M_{n,GPC}$ = 4.7 kDa, M_w/M_n = 1.06, Figure 2b). ^{1}H NMR ($CDCl_3$, δ, ppm, TMS): 3.69−3.43 (450H, $-OCH_2CH_2-$ of PEO main chain), 3.26 (3H, CH_3O-), and 1.84 (6H, $-C(CH_3)_2-$Br).

Preparation of PEO-*b*-PGMA Diblock Copolymer (2). PEO_{113}-*b*-PGMA diblock copolymer was prepared by the ATRP of GMA using PEO_{113}-Br and CuBr/PMDETA as macroinitiator and catalysts, respectively. PEO_{113}-Br macroinitiator (1.29 g, 0.25 mmol), GMA (3.20 g, 22.5 mmol), PMDETA (87 mg, 0.5 mmol), and anisole (4.5 mL) were added into a reaction flask. The mixture was degassed by three freeze−thaw cycles and backfilled with N_2. After equilibration at 30 °C, CuBr (72 mg, 0.32 mmol) was introduced as a solid to start the polymerization. The reaction solution turned dark green and more viscous as polymerization proceeded. After 6 h, the conversion was about 84% as judged by ^{1}H NMR. The reaction mixture was diluted with 15 mL of THF and exposed to air. After passing through a basic alumina column and removing the solvents on a rotary evaporator, the residues were dissolved in THF and precipitated into an excess of cold diethyl ether. The final product was dried in a vacuum oven overnight at room temperature, yielding a white solid (3.8 g, yield: 85%; $M_{n,GPC}$ = 8.7 kDa, M_w/M_n = 1.19, Figure 2c). ^{1}H NMR ($CDCl_3$, δ, ppm, TMS, Figure 1a): 4.45−4.21 and 3.94−3.74 (CO_2CH_2CHO), 3.74−3.48 ($-OCH_2CH_2-$ of PEO main chain), 3.36−3.16 ($-CHO-$ in epoxide ring), and 2.99−2.58 ($-CH_2O-$ in epoxide ring) (Figure 1a). The actual DP of GMA block was determined to be 75 by ^{1}H NMR analysis. Thus, the product was denoted as PEO_{113}-*b*-$PGMA_{75}$.

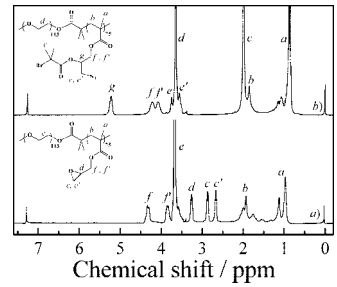

Figure 1. ^{1}H NMR spectra recorded in $CDCl_3$ for (a) PEO_{113}-*b*-$PGMA_{75}$ and (b) PEO_{113}-*b*-[PGMA-(N_3)(*Br*)]$_{75}$.

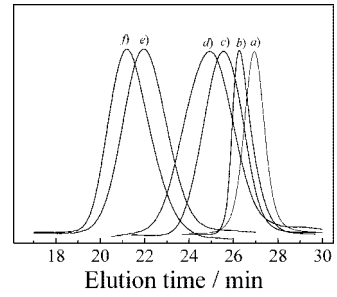

Figure 2. THF GPC traces recorded for (a) *alkynyl*-$PDEA_{21}$, (b) PEO_{113}-*Br*, (c) PEO_{113}-*b*-$PGMA_{75}$, (d) PEO_{113}-*b*-[PGMA-(N_3)(*Br*)]$_{75}$, (e) PEO_{113}-*b*-[PGMA-*g*-(N_3)($PMEO_2MA_{16}$)]$_{75}$, and (f) PEO_{113}-*b*-[PGMA-*g*-$(PDEA)_{21}$-$(PMEO_2MA)_{16}$]$_{75}$.

Preparation of PEO-*b*-[PGMA-(N_3)(*OH*)] (3). Ring-opening of pendent epoxide groups of PGMA segment in PEO_{113}-*b*-$PGMA_{75}$ with NaN_3 yielded PEO_{113}-*b*-[PGMA-(N_3)(*OH*)]$_{75}$.[44] Typical procedures employed for the preparation of **3** were as follows. To a stirred solution of **2** (2.5 g, 11.85 mmol of epoxide moieties) in 100 mL of DMF, NaN_3 (2.28 g, 35 mmol) and ammonium chloride (1.90 g, 35 mmol) were added. The mixture was stirred at 50 °C for 24 h. After removing insoluble salts by filtration, the filtrates were evaporated to dryness. The obtained viscous solid was dissolved in 100 mL of deionized water and dialyzed (MW cutoff, 7.0 kDa) against deionized water for 24 h. Fresh water was replaced approximately every 4 h. The final product was obtained by freeze-drying (2.8 g, yield: 93%). ^{1}H NMR (D_2O, δ, ppm): 4.23−3.94 ($-CO_2CH_2CH-$ and $-CHCH_2N_3$), and 3.74−3.43 ($-CH_2N_3$ and $-OCH_2CH_2-$).

Preparation of PEO_{113}-*b*-[PGMA-(N_3)(*Br*)]$_{75}$ (4). Typical procedures employed for the preparation of **4** were as follows. Into a 100 mL round-bottom flask, **3** (2.5 g, 9.85 mmol hydroxyl moieties) and anhydrous pyridine (40 mL) were charged. After cooling to 0 °C in an ice−water bath, 2-bromoisobutyryl bromide (5.75 g, 25 mmol) was added dropwise over a period of 1 h under magnetic stirring. After the addition was completed, the reaction mixture was stirred at 0 °C for 1 h and then at room temperature for 12 h. The insoluble salts were removed by filtration, and all the solvents were removed on a rotary evaporator. The residues were dissolved in THF and passed through a neutral alumina column, followed by precipitation into an excess of petroleum ether. After drying in a vacuum oven overnight at room temperature, **4** was obtained as a white solid (3.21 g, yield: 81%; $M_{n,GPC}$ = 11.8 kDa, M_w/M_n = 1.21, Figure 2d). ^{1}H NMR ($CDCl_3$, δ, ppm, TMS, Figure 1b): 5.36−5.14 ($-CHCH_2N_3$), 4.36−3.95 ($-CO_2CH_2CH-$), 3.86−3.34 ($-CH_2N_3$ and $-OCH_2CH_2-$), and 2.17−1.89 ($-C(CH_3)_2$Br).

Preparation of PEO-*b*-[PGMA-*g*-(N_3)($PMEO_2MA$)] (5). Typical procedures employed for the preparation of **5** were described below. PEO_{113}-*b*-[PGMA-(N_3)(*Br*)] (**4**, 0.2 g, 0.5 mmol bromine moieties), MEO_2MA (14.1 g, 75.0 mmol), bpy (0.156 g, 1.0 mmol), $CuCl_2$ (6.7 mg, 0.05 mmol), and anisole (28.2 mL) were added into a reaction flask. The mixture was degassed by three freeze−pump−thaw cycles and backfilled with N_2. After heating to 45 °C, CuCl (50 mg, 0.5 mmol) was introduced as a solid into the reaction flask to start the polymerization. The reaction mixture became dark brown and more viscous as polymerization proceeded. After 2 h, tributyltin hydride (0.437 g, 1.5 mmol) was added to the reaction mixture under protection of N_2 flow. After stirring for another 3 h at 45 °C, the reaction mixture was diluted with 15 mL of THF, exposed to air, and then passed through a silica gel column to remove copper catalysts. After removing the solvents on a rotary evaporator, the residues were dissolved in THF and precipitated into an excess of cold diethyl ether. The above dissolution−precipitation cycle was repeated for three times. The final product was dried in a vacuum oven overnight at room temperature, yielding a white viscous solid (1.18 g, yield: 8.3%; $M_{n,GPC}$ = 52.4 kDa, M_w/M_n = 1.17, Figure 2e). The actual DP of $PMEO_2MA$ grafts was determined to be 16 by ^{1}H NMR analysis in $CDCl_3$ (Figure 4a). Thus, the product was denoted as PEO_{113}-*b*-[PGMA-*g*-(N_3)-$(PMEO_2MA)_{16}]_{75}$.

Preparation of *Alkynyl*-PDEA (6). *Alkynyl*-PDEA was obtained by ATRP of DEA monomer using PBIB as initiator. In a typical procedure, PBIB (0.103 g, 0.5 mmol), PMDETA (87 mg, 0.5 mmol), DEA (3.71 g, 20.0 mmol), and IPA (4 mL) were charged into a reaction flask. The mixture was degassed via three freeze−thaw−pump cycles and backfilled with N_2. After equilibration at 30 °C, CuBr (72 mg, 0.5 mmol) was introduced as a solid into the reaction flask to start the polymerization. After 3 h, tributyltin hydride (0.728 g, 2.5 mmol) was added to the reaction mixture under protection of N_2 flow. The mixture was kept stirring for another 3 h at 30 °C. The polymerization was quenched with $CuBr_2$, diluted with 10 mL of THF, and then exposed to air. After passing though a column of neutral alumina to remove copper catalysts and removing all the solvents on a rotary evaporator, the residues were dissolved in THF and precipitated into cold *n*-hexane (−50 °C) to remove residual monomers. The above dissolution−precipitation cycle was repeated twice. After drying in a vacuum oven overnight at room temperature, *alkynyl*-PDEA was obtained as a white viscous solid (1.65 g, yield: 43%; $M_{n,GPC}$ = 3.3 kDa, M_w/M_n = 1.11, Figure 2a). The actual DP of *alkynyl*-PDEA was calculated to be 21 by ^{1}H NMR analysis (Figure 4b). Thus, the product was denoted as *alkynyl*-$PDEA_{21}$.

Preparation of PEO-*b*-[PGMA-*g*-(PDEA)($PMEO_2MA$)] (7). The synthesis of coil−rod double hydrophilic diblock copolymer with asymmetric centipede-shaped polymer brush as the rod segment, PEO_{113}-*b*-[PGMA-*g*-$(PDEA)_{21}(PMEO_2MA)_{16}]_{75}$, was accomplished via the click reaction of **5** with an excess of *alkynyl*-$PDEA_{21}$. In a typical example, **5** (0.125 g, 37.5 μmol azide moieties), **6** (1.51 g, 0.375 mmol alkynyl moieties), PMDETA (65 mg, 0.375 mmol), $CuCl_2$ (0.201 g, 1.5 mmol), and DMF (30 mL) were added to a reaction flask. After one brief freeze−thaw cycle, CuCl (37 mg, 0.375 mmol) was introduced as a solid into the reaction flask. The reaction tube was carefully degassed by three freeze−pump−thaw cycles and backfilled with N_2 and then placed in an oil bath thermostated at 50 °C. After stirring for 36 h, azide-functionalized Merrifield resin (0.94 g, 0.75 mmol azide moieties) was then added. The suspension was kept stirring for another 12 h at 50 °C. After suction filtration, the filtrate was diluted with THF and passed through a basic alumina column to remove copper catalysts. After removing the solvents at reduced pressure, the residues were dissolved in THF and precipitated into an excess of cold *n*-hexane (−50 °C). The final product was dried in a vacuum oven overnight at room temperature, yielding a white viscous solid (0.204 g, yield: 74%; $M_{n,GPC}$ = 85.2 kDa, M_w/M_n = 1.18, Figure 2f). The obtained product was denoted as PEO_{113}-*b*-[PGMA-*g*-$(PDEA)_{21}(PMEO_2MA)_{16}]_{75}$. Molecular parameters of all the intermediate and final products are summarized in Table 1.

Table 1. Summary of Structural Parameters of Polymers Synthesized in This Work

samples	$M_{n,NMR}$ (kDa)[a]	$M_{n,GPC}$ (kDa)[b]	M_w/M_n[b]
PEO_{113}-*Br*	5.1	4.7	1.06
alkynyl-$PDEA_{21}$	4.0	3.3	1.11
PEO_{113}-*b*-$PGMA_{75}$	15.8	8.7	1.19
PEO_{113}-*b*-$[PGMA\text{-}(N_3)(Br)]_{75}$	30.2	11.8	1.21
PEO_{113}-*b*-$[PGMA\text{-}g\text{-}(N_3)(PMEO_2MA)_{16}]_{75}$	250.2	52.4	1.17
PEO_{113}-*b*-$[PGMA\text{-}g\text{-}(PDEA)_{21}(PMEO_2MA)_{16}]_{75}$	464.0[c]	85.2	1.18

[a] Determined by ^{1}H NMR analysis in $CDCl_3$. [b] Molecular weights (M_n) and molecular weight distributions (M_w/M_n) were determined by GPC analysis using THF as the eluent. [c] Considering a "click" grafting efficiency of 71% for PDEA grafts.

Characterization. Nuclear Magnetic Resonance Spectroscopy (NMR). All NMR spectra were recorded on a Bruker AV300 NMR spectrometer (resonance frequency of 300 MHz for ^{1}H) operated in the Fourier transform mode. $CDCl_3$ and D_2O were used as the solvent.

Fourier Transform Infrared Spectroscopy (FT-IR). Fourier transform infrared (FT-IR) spectra were recorded on a Bruker VECTOR-22 IR spectrometer. The spectra were collected at 64 scans with a spectral resolution of 4 cm^{-1}.

Gel Permeation Chromatography (GPC). Molecular weights and molecular weight distributions were determined by gel permeation chromatography (GPC) equipped with a Waters 1515 pump and a Waters 2414 differential refractive index detector (set at 30 °C). It used a series of three linear Styragel columns HT2, HT4, and HT5 at an oven temperature of 45 °C. The eluent was THF at a flow rate of 1.0 mL/min. A series of six polystyrene standards with molecular weights ranging from 800 to 400 000 g/mol were used for calibration.

Ultraviolet−Visible Spectroscopy (UV−vis). Temperature-dependent optical transmittance measurements were performed on a Unico UV/vis 2802PCS spectrophotometer. A thermostatically controlled couvette was employed, and the heating rate was 0.2 °C min^{-1}.

Laser Light Scattering (LLS). A commercial spectrometer (ALV/DLS/SLS-5022F) equipped with a multitau digital time correlator (ALV5000) and a cylindrical 22 mW UNIPHASE He−Ne laser (λ_0 = 632 nm) as the light source was employed for dynamic and static laser light scattering (LLS) measurements. Scattered light was collected at a fixed angle of 90° for duration of ~10 min. Distribution averages and particle size distributions were computed using cumulants analysis and CONTIN routines. All data were averaged over three measurements.

Potentiometric Titrations. The coil−rod double hydrophilic diblock copolymer, PEO_{113}-*b*-$[PGMA\text{-}g\text{-}(PDEA)_{21}(PMEO_2MA)_{16}]_{75}$, was dissolved in deionized at ~pH 3. The solution was titrated by the dropwise addition of aqueous NaOH solution (pH 12.4), and the solution pH was monitored by a Corning Check-Mite pH meter (precalibrated with pH 4.0, 7.0, and 10.0 buffer solutions).

Atomic Force Microscopy (AFM). AFM measurements were performed on a Digital Instrument Multimode Nanoscope IIID operating in the tapping mode under ambient conditions. Silicon cantilever (RFESP) with resonance frequency of ~80 kHz and spring constant of ~3 N/m was used. The set-point amplitude ratio was maintained at 0.7 to minimize sample deformation induced by the tip. For wormlike unimer chains, the sample was prepared by dip coating 0.02 g/L of **7** in aqueous solution at pH 4 and 25 °C onto freshly cleaved mica surface. For $PMEO_2MA$-core and PDMA-core micelles formed from **7** at pH 4 and 40 °C, and pH 10 and 15 °C, the samples were prepared by dip-coating 0.1 g/L aqueous micellar solutions onto freshly cleaved mica surfaces.

Transmission Electron Microscopy (TEM). TEM observations were conducted on a Hitachi H-800 electron microscope at an acceleration voltage of 200 kV. The sample for TEM observations was prepared by placing 10 μL of micellar solution on copper grids coated with thin films of Formvar and carbon successively.

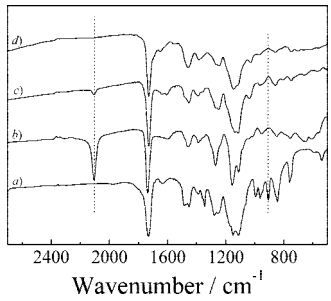

Figure 3. FT-IR spectra recorded for (a) PEO_{113}-*b*-$PGMA_{75}$, (b) PEO_{113}-*b*-[PGMA-(N_3)(*Br*)]$_{75}$, (c) PEO_{113}-*b*-[PGMA-*g*-(N_3)($PMEO_2MA$)$_{16}$]$_{75}$, and (d) PEO_{113}-*b*-[PGMA-*g*-$(PDEA)_{21}$($PMEO_2MA$)$_{16}$]$_{75}$.

Results and Discussion

Synthesis of Coil−Rod Double Hydrophilic Diblock Copolymer (7). Synthetic schemes employed for the preparation of PEO-*b*-[PGMA-*g*-(PDEA)($PMEO_2MA$)] (**7**) are shown in Schemes 1 and 2, employing a combination of ATRP grafting-from technique and high-efficiency click reaction.[68,73] At first, linear PEO_{113}-*b*-$PGMA_{75}$ diblock copolymer (**2**) was prepared via the ATRP of GMA monomer using PEO_{113}-*Br* (**1**) as macroinitiator.[59,74−77] The actual DP of the PGMA block in **2** was determined to be 75 by ^{1}H NMR (Figure 1a), by comparing integration areas of peak *e* in the range of 3.74−3.48 ppm to that of peak *d* in the range of 3.36−3.16 ppm. Typical GPC trace of **2** was shown in Figure 2c, revealing a monomodal and quite symmetric elution peak. In comparison with that of PEO_{113}-*Br* macroinitiator (**1**, Figure 2b), GPC trace of **2** exhibited a clear shift to the higher MW region, indicating an almost quantitative initiating efficiency. In the IR spectrum of **2** (Figure 3a), a strong absorbance peak at 909 cm^{-1} characteristic of epoxide moieties can be clearly observed.

In previous literature reports, ring-opening reactions of PGMA with 2-bromoisobutyric acid[74] and 2-bromobutyric acid[59] have been employed to produce multifunctional ATRP initiators for the synthesis of polymer brushes via the grafting-from approach. In the current study, the ring-opening of pendent epoxide groups of PEO_{113}-*b*-$PGMA_{75}$ with an excess of NaN_3 in the presence of NH_4Cl affords PEO_{113}-*b*-[PGMA-(N_3)(*OH*)]$_{75}$ (**3**) bearing one azide and one hydroxyl functionality on each monomer repeating unit, following similar procedures reported by Matyjaszewski et al.[44] The presence of NH_4Cl can efficiently eliminate side reactions caused by alkoxide anion formed during the ring-opening reaction.[78] Subsequently, the esterification of **3** with 2-bromoisobutyryl bromide yields PEO_{113}-*b*-[PGMA-(N_3)(*Br*)]$_{75}$ (**4**) possessing one azide and one bromine moiety at each GMA repeating unit. To ensure the complete transformation of **3** into **4**, an excess of 2-bromoisobutyryl bromide was used.

GPC analysis of **4** again reveals a monomodal and symmetric elution peak (Figure 2d), indicating that no cross-linking or branching occurred during the ring-opening reaction with NaN_3 and subsequent esterification. A typical ^{1}H NMR spectrum of **4** is shown in Figure 1b, and all signals can be well-assigned according to its chemical structure. In comparison with the ^{1}H NMR spectrum of PEO_{113}-*b*-$PGMA_{75}$ (Figure 1a), resonance signals at 3.36−3.16 ppm (−C*H*O− in epoxide ring) and 2.99−2.58 ppm (−CH_2O− in epoxide ring) characteristic of epoxy moieties completely disappear (Figure 1b). Moreover, the appearance of new peaks *g* (5.36−5.14 ppm, −C*H*CH_2N_3), *e* and *e′* (3.75 and 3.56 ppm, −CH_2N_3), and *c* (2.17−1.89 ppm, −C(CH_3)$_2$Br) can further confirm that all epoxy groups were consumed and participated in the ring-opening reaction with NaN_3 and the subsequent esterification reaction. The integral ratio of peak *c* to those of peaks *f* and *f′* (4.36−3.95 ppm, −CO_2CH_2CH−) in the ^{1}H NMR spectrum of **4** is close to 3:1 after subtracting contributions of PGMA backbone protons in the region of peak *c*. All of these results indicate that azide anion exclusively attacks the less substituted carbon in the pendent epoxide ring, which is in good agreement with those reported in previous works.[44,78] By comparing integral ratio of peaks *c* to that of *d* (−OCH_2CH_2− of PEO), the degree of pendant group functionalization of PGMA segment was calculated to be nearly 100%. The presence of residual azide moieties in **4** can also be evidenced by the presence of characteristic absorbance peak at ∼2100 cm^{-1} in its FT-IR spectrum (Figure 3b). In comparison with that of **2** (Figure 3a), the IR spectrum of **4** reveals the absence of absorbance peak at 909 cm^{-1} characteristic of epoxide moieties. Elemental analysis results of intermediate polymer precursors **2**, **3**, and **4** are summarized in Table S1 (Supporting Information). The measured N/C ratios agree quite well with theoretical values calculated from their chemical structures, and this further verifies the successful preparation of **4**.

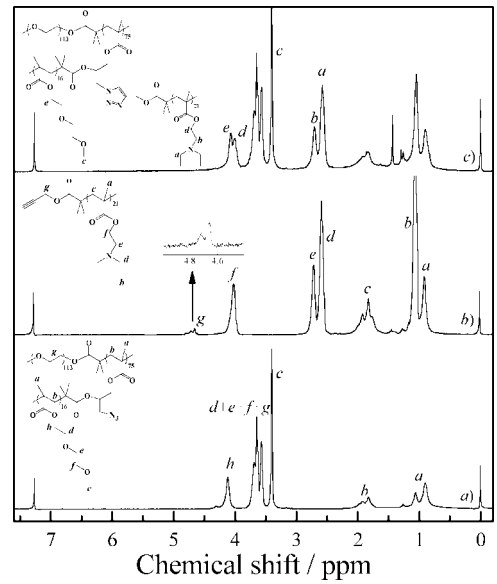

Figure 4. ^{1}H NMR spectra recorded for (a) PEO_{113}-*b*-[PGMA-*g*-(N_3)($PMEO_2MA$)$_{16}$]$_{75}$, (b) *alkynyl*-$PDEA_{21}$, and (c) PEO_{113}-*b*-[PGMA-*g*-$(PDEA)_{21}$($PMEO_2MA$)$_{16}$]$_{75}$ in $CDCl_3$.

Müller et al.[50,79,80] and Matyjaszewski et al.[52,81,82] have reported a series of excellent works concerning the synthesis homopolymer and diblock copolymer brushes via the ATRP grafting-from approach. In the current study, the ATRP of MEO_2MA using **4** as the multifunctional initiator afforded coil−rod diblock copolymer, **5**, with $PMEO_2MA$ brush bearing residual azide moieties at each grafting site as the rod segment. The polymerization was conducted in anisole in the presence of CuCl/$CuCl_2$/bpy at a molar ratio of [MEO_2MA]/[Br] of 150:1. It has been established that the addition of $CuCl_2$ can reduce the concentration of active species and considerably suppress both intra- and intermolecular radical termination to enhance grafting efficiency.[81,83] Moreover, the coupling of bromine-containing macroinitiator **4** with CuCl can further increase the initiating efficiency via halogen exchange mechanism.[84]

As shown in Figure 2e, GPC elution peak of **5** exhibits a clean shift to the higher MW side compared to that of **4**. Moreover, the monomodal and symmetric nature of the elution trace suggests a quite uniform ATRP grafting from the PGMA backbone. A typical ^{1}H NMR spectrum of **5** is shown in Figure 4a. We can apparently observe the overlapping of peaks *g* (−OCH_2CH_2− of PEO main chain), *f* (CH_3OCH_2CH_2O− of $PMEO_2MA$), *e* (CH_3OCH_2CH_2O− of $PMEO_2MA$), and *d* (−CO_2CH_2CH_2O− of $PMEO_2MA$) in the range of 3.8−3.5 ppm, whereas resonance signals of peaks *h* (4.12 ppm, −CO_2CH_2−

of $PMEO_2MA$) and *c* (4.01 ppm, $-OCH_3$ of $PMEO_2MA$) are clearly discernible. In comparison to that of **4** (Figure 1b), we can clearly observe the complete disappearance of peak *g* (5.2 ppm, $-CH_2-CH_2-N_3$) in the ^1H NMR spectrum of **5** (Figure 4a). This strongly suggested the successful grafting of $PMEO_2MA$ side chains via ATRP using **4** as the macroinitiator.[50,79] Although we cannot discern signals characteristic of methylene protons neighboring to azide group from the ^1H NMR spectrum of **5**, the FT-IR spectrum of **5** clearly reveals the presence of absorbance peak characteristic of residual azide moieties (Figure 3c). Assuming a quantitative initiating efficiency and a uniform grafting chain length, the DP that $PMEO_2MA$ grafts can be calculated as follows:

$$DP_{NMR} = \frac{I_c}{I_{d+e+f+g} - 2I_c}\frac{113 \times 4}{75 \times 3}$$

where 113 and 75 denote the DP of PEO and PGMA, respectively. I_c and $I_{d+e+f+g}$ are the integrals of peaks *c* and $d + e + f + g$. The calculation results in a DP_{NMR} of 16. Thus, the product is denoted as PEO_{113}-*b*-[PGMA-*g*-(N_3)($PMEO_2MA$)$_{16}$]$_{75}$.

Monoalkynyl-terminated PDEA, *alkynyl*-PDEA (**6**), was prepared by the ATRP of DEA monomer using PBIB as the initiator followed by dehalogenation with tributyltin hydride.[85] A typical GPC trace of **6** is shown in Figure 2a, yielding an M_n of 3.3 kDa and an M_w/M_n of 1.11. The actual DP of **6** was calculated to be 21 from ^1H NMR analysis by comparing integration areas of peak *f* in the range of 4.22−3.91 ppm to that of peak *g* in the range of 4.83−4.60 ppm (Figure 4b).

In the next step, the click reaction of PEO_{113}-*b*-[PGMA-*g*-(N_3)($PMEO_2MA$)$_{16}$]$_{75}$ (**5**) with an excess of *alkynyl*-$PDEA_{21}$ affords coil−rod double hydrophilic diblock copolymer with dually responsive asymmetric centipede-shaped polymer brush as the rod segment, PEO_{113}-*b*-[PGMA-*g*-($PDEA_{21}$)-($PMEO_2MA$)$_{16}$]$_{75}$ (**7**). It is known that click reaction condition is also applicable to the ATRP process, which will generate radicals from halide end groups of $PMEO_2MA$ side chains and lead to unwanted inter- and intramolecular branching and crosslinking.[83] To solve this problem, **5** has also been subjected to in situ dehalogenation in the presence of an excess of tributyltin hydride.[85] To enhance the "click" grafting efficiency, a 10 molar excess of *alkynyl*-$PDEA_{21}$ (**6**) was employed and the reaction was conducted at 50 °C for 36 h. The removal of excess **6** has been facilely achieved by clicking onto azido-functionalized Merrifield resin followed by a simple filtration step.[70] Figure 3d shows the FT-IR spectrum of the purified product. Compared to that of **5** (Figure 3c), we can clearly observe that the intensity of characteristic azide absorbance peak at ~2100 cm^{-1} is reduced to a large extent after click reaction, suggesting that the vast majority of azide groups in **5** has participated in the click grafting reaction with *alkynyl*-$PDEA_{21}$. GPC analysis further supports the successful preparation of coil−rod diblock copolymer with asymmetric centipede-shaped polymer brush as the rod segment. Compared to that of **5** (Figure 2e), the GPC trace of **7** exhibits a clear shift to the higher MW region, affording a M_n of 85.2 kDa and an M_w/M_n of 1.18 (Figure 2f).

Figure 4c shows ^1H NMR spectrum of **7** together with the peak assignments. All resonance signals characteristic of PDEA and $PMEO_2MA$ side grafts are clearly discernible. The "click" grafting efficiency, $Y_{grafting}$, of PDEA side chains can be calculated as follows:

$$Y_{grafting} = \frac{I_{a+b}}{I_c}\frac{3 \times 16}{6 \times 21}$$

where 16 and 21 denote DPs of $PMEO_2MA$ and PDEA grafts, respectively. I_c and I_{a+b} are the integrals of peaks *c* and $a + b$,

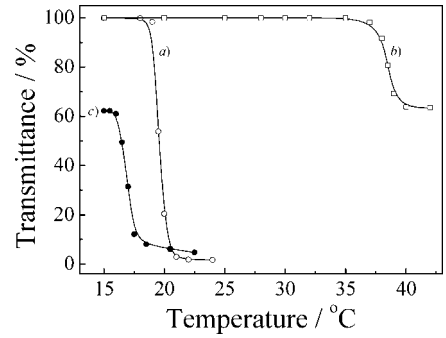

Figure 5. Temperature dependence of optical transmittance at 700 nm obtained for 1.0 wt % aqueous solutions of (a) PEO_{113}-*b*-[PGMA-*g*-(N_3)($PMEO_2MA_{16}$)]$_{75}$ at pH 7 and PEO_{113}-*b*-[PGMA-*g*-($PDEA$)$_{21}$-($PMEO_2MA$)$_{16}$]$_{75}$ at (b) pH 4 and (c) pH 10.

which are characteristic of $PMEO_2MA$ (CH_3O-) and PDEA ($-CO_2CH_2CH_2N-$ and $-N(CH_2CH_3)_2$)), respectively. Thus, a click grafting efficiency of 71% is obtained. All results presented above clearly demonstrated that well-defined coil−rod diblock copolymer with asymmetric centipede-shaped polymer brush as the rod segment, PEO-*b*-[PGMA-*g*-(PDEA)($PMEO_2MA$)] (**7**), has been successfully prepared via a combination of ATRP and click reaction. Static laser light scattering (SLS) analysis of **7** gave a weight-average molar mass, $M_{w,SLS}$, of 7.1×10^5 g/mol (Figure S1), which is in reasonable agreement with that calculated from ^1H NMR (Table 1). Table 1 summarizes structural parameters of all the intermediate and final polymer products synthesized in this work.

Schizophrenic" Aggregation of PEO_{113}-*b*-[PGMA-*g*-($PDEA$)$_{21}$-($PMEO_2MA$)$_{16}$]$_{75}$ (7). It is well-known that $PMEO_2MA$ homopolymer dissolves in cold and dilute aqueous solution but gets insoluble above ~26 °C due to its lower critical solution temperature (LCST) phase behavior.[52,86] On the other hand, PDEA homopolymer is a weak polybase and its conjugated acid possesses a pK_a of ~7.3. It is water-insoluble at neutral or alkaline pH, whereas below pH 6, it is soluble as a weak cationic polyelectrolyte due to protonation of tertiary amine residues.[87−91] Thus, we can expect that the rod segment of coil−rod diblock copolymer, PEO_{113}-*b*-[PGMA-*g*-($PDEA$)$_{21}$($PMEO_2MA$)$_{16}$]$_{75}$ (**7**), i.e., asymmetric centipede-shaped polymer brush bearing two types of PDEA and $PMEO_2MA$ grafts, should exhibit pH- and thermo-responsive "schizophrenic" aggregation behavior in aqueous solution (Scheme 2). It is worth noting that PEO coil segment in **7** remains soluble in aqueous solution independent of solution pH and temperatures in the range investigated, and it will provide extra stabilization for the formed supramolecular aggregates.

Schmidt et al.[92] investigated the thermo-responsive collapse of single poly(*N*-isopropylacrylamide) (PNIPAM) brush in dilute aqueous solution, which is accompanied by a cylindrical brush-to-sphere transition above the phase transition temperature. Recently, Matyjaszewski et al.[52] reported the thermal phase transition behavior of $PMEO_2MA$ and P(MEO_2MA-*co*-MEO_3MA) brushes, where MEO_3MA is tri(ethylene oxide) methyl ether methacrylate). Temperature-dependent optical transmittance revealed a LCST value of 22 °C for $PMEO_2MA$ brush and increasing LCST values with increasing MEO_3MA contents for P(MEO_2MA-*co*-MEO_3MA) copolymer brush. In the current study, the LCST was determined to be 19 °C by temperature-dependent optical transmittance for PEO_{113}-*b*-[PGMA-*g*-(N_3)($PMEO_2MA$)$_{16}$]$_{75}$ (**5**) in aqueous solution at a concentration of 1.0 wt % and pH 7 (Figure 5a).

PEO_{113}-*b*-[PGMA-*g*-($PDEA$)$_{21}$($PMEO_2MA$)$_{16}$]$_{75}$ (**7**) is directly soluble in acidic media at room temperature. Dynamic LLS measurement reveals quite low scattering intensity and an average hydrodynamic radius, $\langle R_h \rangle$, of ~7.6 nm for **7** in aqueous

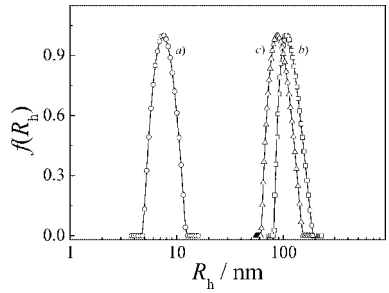

Figure 6. Hydrodynamic radius distribution, $f(R_h)$, obtained for 1.0 g/L aqueous solutions of PEO_{113}-*b*-[PGMA-*g*-$(PDEA)_{21}(PMEO_2MA)_{16}]_{75}$ at (a) pH 4 and 25 °C, (b) pH 4 and 40 °C, and (c) pH 10 and 15 °C.

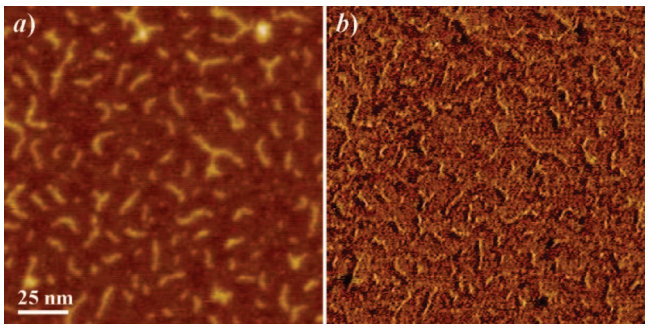

Figure 7. Typical AFM (a) height image (*Z* range is 5 nm) and (b) phase image obtained by dip-coating 0.02 g/L aqueous solution of PEO_{113}-*b*-[PGMA-*g*-$(PDEA)_{21}(PMEO_2MA)_{16}]_{75}$ at pH 7 onto mica at 25 °C.

solution at pH 4 and 25 °C (Figure 6a), confirming a molecularly dissolved state. The conformation of **7** at a unimer state was directly checked by AFM observation, which typically revealed a stretched wormlike morphology (Figure 7). The average length of these wormlike nanostructures is determined to be ~16 nm, which is generally comparable to the calculated end-to-end distance of fully extended PGMA-based rod segment (~18.8 nm). This suggests that the coil−rod diblock copolymer chains exist in a cylindrical conformation, which is quite expected. At pH 4 and 25 °C, PDEA grafts are fully protonated and remain soluble in the whole temperature range. However, heating the aqueous solution can still induce the thermal phase transition of $PMEO_2MA$ grafts, accompanied by thermo-induced aggregation due to the double hydrophilic nature of rod segment. As revealed by temperature-dependent optical transmittance obtained for **7** in aqueous solution at pH 4 (Figure 5b), the phase transition temperature was determined to be ~37 °C. The much higher thermal phase transition temperature compared to those of $PMEO_2MA$ brushes[52] and **5** can be ascribed to the presence and close neighboring of highly hydrophilic protonated PDEA grafts.

Upon heating to above 37 °C, the aqueous solution of **7** at pH 4 typically exhibit a bluish tinge characteristic of colloidal dispersions, suggesting thermo-induced micellization. On the basis of chemical intuition, the formed micelles at elevated temperatures should possess a core consisting of hydrophobic $PMEO_2MA$ and a hybrid corona of PEO and well-solvated PDEA sequences (Scheme 2). Figure 6b shows typical plot of hydrodynamic radius distribution, $f(R_h)$, obtained for **7** at pH 4 and 40 °C, leading to $\langle R_h \rangle$ of 107 nm and μ_2/Γ^2 of 0.11.

Figure 8a shows potentiometric titration of **7** in aqueous solution. It is found that the coil−rod double hydrophilic block copolymer buffers the solution in the pH range of 6−8. The overall degree of protonation (α) of tertiary amine residues decreases from unity to zero as the solution pH increases from

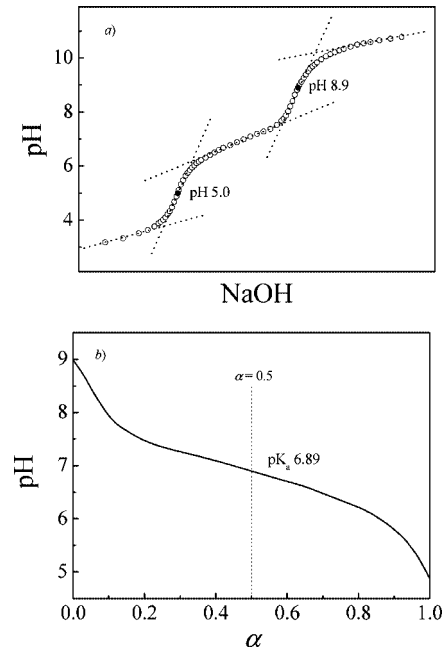

Figure 8. (a) Potentiometric titration curve obtained for 2.0 g/L aqueous solution of PEO_{113}-*b*-[PGMA-*g*-$(PDEA)_{21}(PMEO_2MA)_{16}]_{75}$. (b) Same titration curve of as in (a) with the *x*-axis expressed in terms of the mean degree of protonation, α.

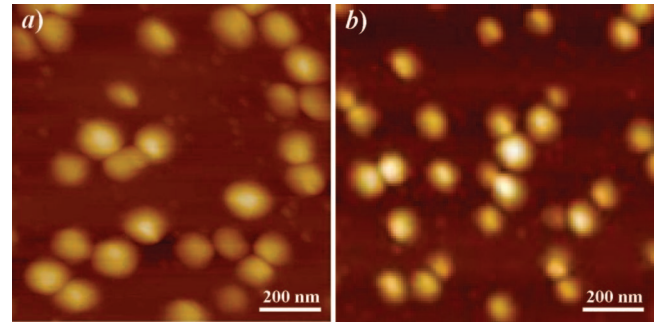

Figure 9. Typical AFM height images obtained by dip coating 0.1 g/L aqueous solutions of PEO_{113}-*b*-[PGMA-*g*-$(PDEA)_{21}(PMEO_2MA)_{16}]_{75}$ onto mica at (a) pH 4 and 40 °C and (b) pH 10 and 15 °C, respectively. *Z* ranges for both images are 30 nm.

5.0 to 8.9. The pK_a was thus determined to be 6.9 for **7**, which is slightly lower than that of PDEA homopolymer (~7.3). This might be due to the local high chain density of PDEA sequences within the asymmetric centipede-shaped polymer brush.[93,94] Starting from the unimer state for **7** at pH 4 and 15 °C, PDEA-core micelles can be fabricated via pH changes (Scheme 2). Upon adjusting to pH higher than 8, the initially clear solution exhibits a characteristic bluish tinge, which is just similar to that observed at pH 4 and elevated temperatures. This suggests the formation of another type of aggregates with hydrophobic PDEA as the core and well-solvated $PMEO_2MA$ sequences as the corona (Scheme 2). Figure 6c shows a typical plot of hydrodynamic radius distribution, $f(R_h)$, obtained for the aqueous solution of **7** at pH 10 and 15 °C, revealing $\langle R_h \rangle$ of 87 nm and μ_2/Γ^2 of 0.09. Figure 5b shows temperature-dependent optical transmittance for the aqueous solution of **7** at pH 10, revealing a phase transition temperature of ~16 °C. Such a low critical transition temperature compared to those of **7** and $PMEO_2MA$ homopolymer should be ascribed to the fact that now $PMEO_2MA$ coronas were covalently grafted on hydrophobic cores within the formed PDEA-core micelles.

AFM and TEM observations have been performed to examine the actual morphologies of thermo-induced $PMEO_2MA$-core

micelles and pH-induced PDEA-core micelles from PEO_{113}-*b*-[PGMA-*g*-$(PDEA)_{21}(PMEO_2MA)_{16}]_{75}$ (Figure 9, Figure S2). Both AFM images clearly reveal the presence of spherical nanoparticles with diameters in the range of 110−140 and 80−120 nm for $PMEO_2MA$-core micelles and PDEA-core micelles, respectively. The results are in reasonable agreement with those determined by dynamic LLS (Figure 6), considering that AFM determines micellar dimensions in the dry state, whereas dynamic LLS reports intensity-average dimension of aggregates in solution and it contains the contribution of well-solvated coronas. The spherical morphologies of both types of aggregates have also been confirmed by TEM analysis (Figure S2), and the sizes of aggregates were quite comparable to those obtained from AFM.

Conclusion

Well-defined coil−rod double hydrophilic diblock copolymer with multiresponsive asymmetric centipede-shaped polymer brush as the rod segment, PEO_{113}-*b*-[PGMA-*g*-$(PDEA)_{21}$-$(PMEO_2MA)_{16}]_{75}$, was synthesized via a combination of ATRP and click reaction. The linear diblock precursor, PEO_{113}-*b*-[PGMA-$(N_3)(Br)]_{75}$ (**4**), bearing one bromine and one azide moieties on each monomer repeating unit of PGMA segment was prepared at first. The subsequent ATRP of MEO_2MA monomer using PEO_{113}-*b*-[PGMA-$(N_3)(Br)]_{75}$ as the multifunctional initiator afforded PEO_{113}-*b*-[PGMA-*g*-$(PDEA)_{21}(PMEO_2MA)_{16}]_{75}$ (**5**). In the final step, monoalkynyl-terminated PDEA was covalently attached to **5** via click reaction with a grafting efficiency of 71%, leading to PEO_{113}-*b*-[PGMA-*g*-$(PDEA)_{21}(PMEO_2MA)_{16}]_{75}$ (**7**). The obtained coil−rod diblock copolymer **7** exhibits pH- and thermo-responsive supramolecular aggregation behavior in aqueous solution due to the presence of dually responsive PDEA and $PMEO_2MA$ grafts with the rod segment, which has been characterized via a combination of temperature-dependent optical transmittance, dynamic LLS, AFM, and TEM. Moreover, the multiresponsive switching between wormlike unimers and two types of micellar aggregates can be facilely controlled by solution pH and temperatures, which augurs well for their potential applications as smart nanocarriers for target drug delivery and controlled release.

Acknowledgment. The financial support of National Natural Scientific Foundation of China (NNSFC) Projects (20534020, 20674079, and 20874092), Specialized Research Fund for the Doctoral Program of Higher Education (SRFDP), and the Program for Changjiang Scholars and Innovative Research Team in University (PCSIRT) is gratefully acknowledged.

Supporting Information Available: Elemental analysis, SLS, and TEM characterization results. This material is available free of charge via the Internet at http://pubs.acs.org.

References and Notes

(1) Alarcon, C. D. H.; Pennadam, S.; Alexander, C. *Chem. Soc. Rev.* **2005**, *34*, 276–285.
(2) Cunliffe, D.; Alarcon, C. D.; Peters, V.; Smith, J. R.; Alexander, C. *Langmuir* **2003**, *19*, 2888–2899.
(3) Hoffmann, J.; Plotner, M.; Kuckling, D.; Fischer, W. J. *Sens. Actuators, A* **1999**, *77*, 139–144.
(4) Ista, L. K.; Lopez, G. P. *J. Ind. Microbiol. Biotechnol.* **1998**, *20*, 121–125.
(5) Kim, S. J.; Park, S. J.; Lee, S. M.; Lee, Y. M.; Kim, H. C.; Kim, S. I. *J. Appl. Polym. Sci.* **2003**, *89*, 890–894.
(6) Liu, S. Y.; Armes, S. P. *Langmuir* **2003**, *19*, 4432–4438.
(7) Nandkumar, M. A.; Yamato, M.; Kushida, A.; Konno, C.; Hirose, M.; Kikuchi, A.; Okano, T. *Biomaterials* **2002**, *23*, 1121–1130.
(8) Raula, J.; Shan, J.; Nuopponen, M.; Niskanen, A.; Jiang, H.; Kauppinen, E. I.; Tenhu, H. *Langmuir* **2003**, *19*, 3499–3504.
(9) Riess, G. *Prog. Polym. Sci.* **2003**, *28*, 1107–1170.
(10) Rodriguez-Hernandez, J.; Checot, F.; Gnanou, Y.; Lecommandoux, S. *Prog. Polym. Sci.* **2005**, *30*, 691–724.
(11) Schild, H. G. *Prog. Polym. Sci.* **1992**, *17*, 163–249.
(12) Urry, D. W. *Biopolymers* **1998**, *47*, 167–178.
(13) Yamato, M.; Utsumi, M.; Kushida, A.; Konno, C.; Kikuchi, A.; Okano, T. *Tissue Eng.* **2001**, *7*, 473–480.
(14) Andre, X.; Zhang, M. F.; Muller, A. H. E. *Macromol. Rapid Commun.* **2005**, *26*, 558–563.
(15) Arotcarena, M.; Heise, B.; Ishaya, S.; Laschewsky, A. *J. Am. Chem. Soc.* **2002**, *124*, 3787–3793.
(16) Butun, V.; Billingham, N. C.; Armes, S. P. *J. Am. Chem. Soc.* **1998**, *120*, 11818–11819.
(17) Colfen, H. *Macromol. Rapid Commun.* **2001**, *22*, 219–252.
(18) Dai, S.; Ravi, P.; Tam, K. C.; Mao, B. W.; Gang, L. H. *Langmuir* **2003**, *19*, 5175–5177.
(19) Gan, L. H.; Ravi, P.; Mao, B. W.; Tam, K. C. *J. Polym. Sci., Part A: Polym. Chem.* **2003**, *41*, 2688–2695.
(20) Gil, E. S.; Hudson, S. A. *Prog. Polym. Sci.* **2004**, *29*, 1173–1222.
(21) Gohy, J. F. *Adv. Polym. Sci.* **2005**, *190*, 65–136.
(22) Liu, S. Y.; Armes, S. P. *Angew. Chem., Int. Ed.* **2002**, *41*, 1413–1416.
(23) Poe, G. D.; McCormick, C. L. *J. Polym. Sci., Part A: Polym. Chem.* **2004**, *42*, 2520–2533.
(24) Rodriguez-Hernandez, J.; Lecommandoux, S. *J. Am. Chem. Soc.* **2005**, *127*, 2026–2027.
(25) Schilli, C. M.; Zhang, M. F.; Rizzardo, E.; Thang, S. H.; Chong, Y. K.; Edwards, K.; Karlsson, G.; Muller, A. H. E. *Macromolecules* **2004**, *37*, 7861–7866.
(26) Sumerlin, B. S.; Lowe, A. B.; Thomas, D. B.; Convertine, A. J.; Donovan, M. S.; McCormick, C. L. *J. Polym. Sci., Part A: Polym. Chem.* **2004**, *42*, 1724–1734.
(27) Virtanen, J.; Arotcarena, M.; Heise, B.; Ishaya, S.; Laschewsky, A.; Tenhu, H. *Langmuir* **2002**, *18*, 5360–5365.
(28) Weaver, J. V. M.; Armes, S. P.; Liu, S. Y. *Macromolecules* **2003**, *36*, 9994–9998.
(29) Forster, S.; Plantenberg, T. *Angew. Chem., Int. Ed.* **2002**, *41*, 689–714.
(30) Ramzi, A.; Prager, M.; Richter, D.; Efstratiadis, V.; Hadjichristidis, N.; Young, R. N.; Allgaier, J. B. *Macromolecules* **1997**, *30*, 7171–7182.
(31) Pispas, S.; Hadjichristidis, N.; Potemkin, I.; Khokhlov, A. *Macromolecules* **2000**, *33*, 1741–1746.
(32) Sotiriou, K.; Nannou, A.; Velis, G.; Pispas, S. *Macromolecules* **2002**, *35*, 4106–4112.
(33) Yun, J. P.; Faust, R.; Szilagyi, L. S.; Keki, S.; Zsuga, M. *Macromolecules* **2003**, *36*, 1717–1723.
(34) Cai, Y. L.; Burguiere, C.; Armes, S. P. *Chem. Commun.* **2004**, 802–803.
(35) Cai, Y. L.; Tang, Y. Q.; Armes, S. P. *Macromolecules* **2004**, *37*, 9728–9737.
(36) Cai, Y. L.; Armes, S. P. *Macromolecules* **2005**, *38*, 271–279.
(37) Ge, Z. S.; Cai, Y. L.; Yin, J.; Zhu, Z. Y.; Rao, J. Y.; Liu, S. Y. *Langmuir* **2007**, *23*, 1114–1122.
(38) Xu, J.; Ge, Z. S.; Zhu, Z. Y.; Luo, S. Z.; Liu, H. W.; Liu, S. Y. *Macromolecules* **2006**, *39*, 8178–8185.
(39) Zhang, M. F.; Muller, A. H. E. *J. Polym. Sci., Part A: Polym. Chem.* **2005**, *43*, 3461–3481.
(40) Sheiko, S. S.; Sumerlin, B. S.; Matyjaszewski, K. *Prog. Polym. Sci.* **2008**, *33*, 759–785.
(41) Feng, C.; Shen, Z.; Gu, L. N.; Zhang, S.; Li, L. T.; Lu, G. L.; Huang, X. Y. *J. Polym. Sci., Part A: Polym. Chem.* **2008**, *46*, 5638–5651.
(42) He, L. H.; Zhang, Y. H.; Ren, L. X.; Chen, Y. M.; Wei, H.; Wang, D. J. *Macromol. Chem. Phys.* **2006**, *207*, 684–693.
(43) Beers, K. L.; Gaynor, S. G.; Matyjaszewski, K.; Sheiko, S. S.; Moller, M. *Macromolecules* **1998**, *31*, 9413–9415.
(44) Tsarevsky, N. V.; Bencherif, S. A.; Matyjaszewski, K. *Macromolecules* **2007**, *40*, 4439–4445.
(45) Yang, S. K.; Weck, M. *Macromolecules* **2008**, *41*, 346–351.
(46) Zhu, H.; Deng, G. H.; Chen, Y. M. *Polymer* **2008**, *49*, 405–411.
(47) Zhang, Y. H.; Xu, Z. Z.; Li, X. K.; Chen, Y. M. *J. Polym. Sci., Part A: Polym. Chem.* **2007**, *45*, 3994–4001.
(48) Zhang, Y. H.; Xu, Z. Z.; Li, X. K.; Chen, Y. M. *J. Polym. Sci., Part A: Polym. Chem.* **2007**, *45*, 3303–3310.
(49) Borner, H. G.; Beers, K.; Matyjaszewski, K.; Sheiko, S. S.; Moller, M. *Macromolecules* **2001**, *34*, 4375–4383.
(50) Cheng, G. L.; Boker, A.; Zhang, M. F.; Krausch, G.; Muller, A. H. E. *Macromolecules* **2001**, *34*, 6883–6888.
(51) Cheng, Z. P.; Zhu, X. L.; Fu, G. D.; Kang, E. T.; Neoh, K. G. *Macromolecules* **2005**, *38*, 7187–7192.
(52) Yamamoto, S.; Pietrasik, J.; Matyjaszewski, K. *Macromolecules* **2007**, *40*, 9348–9353.
(53) Yuan, W. Z.; Yuan, J. Y.; Zhang, F. B.; Xie, X. M.; Pan, C. Y. *Macromolecules* **2007**, *40*, 9094–9102.
(54) Gu, L. N.; Shen, Z.; Feng, C.; Li, Y. G.; Lu, G. L.; Huang, X. Y. *J. Polym. Sci., Part A: Polym. Chem.* **2008**, *46*, 4056–4069.

(55) Gu, L. N.; Shen, Z.; Zhang, S.; Lu, G. L.; Zhang, X. H.; Huang, X. Y. *Macromolecules* **2007**, *40*, 4486–4493.
(56) Iatrou, H.; Mays, J. W.; Hadjichristidis, N. *Macromolecules* **1998**, *31*, 6697–6701.
(57) Li, A. X.; Lu, Z. J.; Zhou, Q. F.; Qiu, F.; Yang, Y. L. *J. Polym. Sci., Part A: Polym. Chem.* **2006**, *44*, 3942–3946.
(58) Ryu, S. W.; Asada, H.; Hirao, A. *Macromolecules* **2002**, *35*, 7191–7199.
(59) Shi, G. Y.; Zou, P.; Pan, C. Y. *J. Polym. Sci., Part A: Polym. Chem.* **2008**, *46*, 5580–5591.
(60) In, I.; La, Y. H.; Park, S. M.; Nealey, P. F.; Gopalan, P. *Langmuir* **2006**, *22*, 7855–7860.
(61) Neugebauer, D.; Zhang, Y.; Pakula, T.; Matyjaszewski, K. *Macromolecules* **2005**, *38*, 8687–8693.
(62) Helms, B.; Mynar, J. L.; Hawker, C. J.; Frechet, J. M. J. *J. Am. Chem. Soc.* **2004**, *126*, 15020–15021.
(63) Mynar, J. L.; Choi, T. L.; Yoshida, M.; Kim, V.; Hawker, C. J.; Frechet, J. M. J. *Chem. Commun.* **2005**, 5169–5171.
(64) Gao, H. F.; Matyjaszewski, K. *J. Am. Chem. Soc.* **2007**, *129*, 6633–6639.
(65) Luo, X. L.; Wang, G. W.; Pang, X. C.; Huang, J. L. *Macromolecules* **2008**, *41*, 2315–2317.
(66) Cheng, C.; Qi, K.; Khoshdel, E.; Wooley, K. L. *J. Am. Chem. Soc.* **2006**, *128*, 6808–6809.
(67) Shi, Y.; Fu, Z. F.; Yang, W. T. *J. Polym. Sci., Part A: Polym. Chem.* **2006**, *44*, 2069–2075.
(68) Rostovtsev, V. V.; Green, L. G.; Fokin, V. V.; Sharpless, K. B. *Angew. Chem., Int. Ed.* **2002**, *41*, 2596–2599.
(69) Sharpless, K. B. *Angew. Chem., Int. Ed.* **2002**, *41*, 2024–2032.
(70) Chen, G. J.; Tao, L.; Mantovani, G.; Ladmiral, V.; Burt, D. P.; Macpherson, J. V.; Haddleton, D. M. *Soft Matter* **2007**, *3*, 732–739.
(71) Tsarevsky, N. V.; Sumerlin, B. S.; Matyjaszewski, K. *Macromolecules* **2005**, *38*, 3558–3561.
(72) Laurent, B. A.; Grayson, S. M. *J. Am. Chem. Soc.* **2006**, *128*, 4238–4239.
(73) Tornoe, C. W.; Christensen, C.; Meldal, M. *J. Org. Chem.* **2002**, *67*, 3057–3064.
(74) Fu, G. D.; Phua, S. J.; Kang, E. T.; Neoh, K. G. *Macromolecules* **2005**, *38*, 2612–2619.
(75) Jiang, P.; Shi, Y.; Liu, P. S.; Cai, Y. L. *J. Polym. Sci., Part A: Polym. Chem.* **2007**, *45*, 2947–2958.
(76) Yin, H. W.; Zheng, H. M.; Lu, L. C.; Liu, P. S.; Cai, Y. L. *J. Polym. Sci., Part A: Polym. Chem.* **2007**, *45*, 5091–5102.
(77) Zhu, J.; Zhou, D.; Zhu, X. L.; Chen, G. J. *J. Polym. Sci., Part A: Polym. Chem.* **2004**, *42*, 2558–2565.
(78) Chini, M.; Crotti, P.; Macchia, F. *Tetrahedron Lett.* **1990**, *31*, 5641–5644.
(79) Xu, Y. Y.; Bolisetty, S.; Drechsler, M.; Fang, B.; Yuan, J. Y.; Ballauff, M.; Muller, A. H. E. *Polymer* **2008**, *49*, 3957–3964.
(80) Yuan, J. Y.; Xu, Y. Y.; Walther, A.; Bolisetty, S.; Schumacher, M.; Schmalz, H.; Ballauff, M.; Muller, A. H. E. *Nat. Mater.* **2008**, *7*, 718–722.
(81) Sumerlin, B. S.; Neugebauer, D.; Matyjaszewski, K. *Macromolecules* **2005**, *38*, 702–708.
(82) Yamamoto, S.; Pietrasik, J.; Matyjaszewski, K. *Macromolecules* **2008**, *41*, 7013–7020.
(83) Matyjaszewski, K.; Xia, J. H. *Chem. Rev.* **2001**, *101*, 2921–2990.
(84) Matyjaszewski, K.; Shipp, D. A.; Wang, J. L.; Grimaud, T.; Patten, T. E. *Macromolecules* **1998**, *31*, 6836–6840.
(85) Coessens, V.; Matyjaszewski, K. *Macromol. Rapid Commun.* **1999**, *20*, 66–70.
(86) Lutz, J. F. *J. Polym. Sci., Part A: Polym. Chem.* **2008**, *46*, 3459–3470.
(87) Butun, V.; Billingham, N. C.; Armes, S. P. *Chem. Commun.* **1997**, 671–672.
(88) Lee, A. S.; Gast, A. P.; Butun, V.; Armes, S. P. *Macromolecules* **1999**, *32*, 4302–4310.
(89) Vamvakaki, M.; Billingham, N. C.; Armes, S. P. *Macromolecules* **1999**, *32*, 2088–2090.
(90) Butun, V.; Armes, S. P.; Billingham, N. C. *Polymer* **2001**, *42*, 5993–6008.
(91) Liu, S. Y.; Weaver, J. V. M.; Tang, Y. Q.; Billingham, N. C.; Armes, S. P.; Tribe, K. *Macromolecules* **2002**, *35*, 6121–6131.
(92) Li, C. M.; Gunari, N.; Fischer, K.; Janshoff, A.; Schmidt, M. *Angew. Chem., Int. Ed.* **2004**, *43*, 1101–1104.
(93) Plamper, F. A.; Ruppel, M.; Schmalz, A.; Borisov, O.; Ballauff, M.; Muller, A. H. E. *Macromolecules* **2007**, *40*, 8361–8366.
(94) Plamper, F. A.; Becker, H.; Lanzendorfer, M.; Patel, M.; Wittemann, A.; Ballauf, M.; Muller, A. H. E. *Macromol. Chem. Phys.* **2005**, *206*, 1813–1825.

MA900165Z